



<b>Title</b>	A 34-year simulation of wind generation potential for Ireland and the impact of large-scale atmospheric pressure patterns
<b>Authors(s)</b>	Cradden, Lucy C., McDermott, Frank, Zubiate, Laura, Sweeney, Conor, O'Malley, Mark
<b>Publication date</b>	2017-06
<b>Publication information</b>	Cradden, Lucy C., Frank McDermott, Laura Zubiate, Conor Sweeney, and Mark O'Malley. "A 34-Year Simulation of Wind Generation Potential for Ireland and the Impact of Large-Scale Atmospheric Pressure Patterns." Elsevier, June 2017. <a href="https://doi.org/10.1016/j.renene.2016.12.079">https://doi.org/10.1016/j.renene.2016.12.079</a>
<b>Publisher</b>	Elsevier
<b>Item record/more information</b>	<a href="http://hdl.handle.net/10197/8402">http://hdl.handle.net/10197/8402</a>
<b>Publisher's statement</b>	This is the author's version of a work that was accepted for publication in Renewable Energy. Changes resulting from the publishing process, such as peer review, editing, corrections, structural formatting, and other quality control mechanisms may not be reflected in this document. Changes may have been made to this work since it was submitted for publication. A definitive version was subsequently published in Renewable Energy (VOL 106, ISSUE 2017, (2017)) DOI: 10.1016/j.renene.2016.12.079.
<b>Publisher's version (DOI)</b>	10.1016/j.renene.2016.12.079

Downloaded 2026-05-01 16:17:08

The UCD community has made this article openly available. Please share how this access benefits you. Your story matters! (@ucd\_oa)



© Some rights reserved. For more information

1 A 34-year simulation of wind generation potential for Ireland and the  
2 impact of large-scale atmospheric pressure patterns

3

4 Lucy C. Cradden\*, Frank McDermott, Laura Zubiate, Conor Sweeney, Mark O'Malley

5 **Abstract**

6 To study climate-related aspects of power system operation with large volumes of wind generation,  
7 data with sufficiently wide temporal and spatial scope are required. The relative youth of the wind  
8 industry means that long-term data from real systems are not available. Here, a detailed aggregated  
9 wind power generation model is developed for the Republic of Ireland using MERRA reanalysis wind  
10 speed data and verified against measured wind production data for the period 2001-2014. The  
11 model is most successful in representing aggregate power output in the middle years of this period,  
12 after the total installed capacity had reached around 500MW. Variability on scales of greater than 6  
13 hours is captured well by the model; one additional higher resolution wind dataset was found to  
14 improve the representation of higher frequency variability. Finally, the model is used to hindcast  
15 hypothetical aggregate wind production over the 34-year period 1980-2013, based on existing  
16 installed wind capacity. A relationship is found between several of the production characteristics,  
17 including capacity factor, ramping and persistence, and two large-scale atmospheric patterns – the  
18 North Atlantic Oscillation and the East Atlantic Pattern.

19 **Keywords**

20 Wind power; MERRA reanalysis; North Atlantic Oscillation; East Atlantic Pattern

21

22 \*Corresponding author

23 Dr. Lucy Catherine Cradden

24 School of Earth Sciences

25 UCD Energy Institute

26 University College Dublin

27 Belfield,

28 Dublin 4

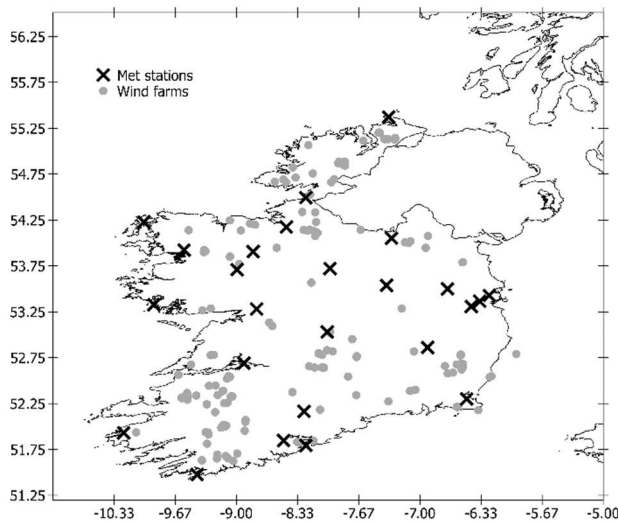
29 Email: lucy.cradden@ucd.ie

## 30 1. Background

31 'Generation potential models' have been used in a number of studies to model hypothetical wind  
32 power generation for a range of purposes. Where analysis of production characteristics in a high  
33 wind penetration scenario is required, a simple resampling or scaling of existing power production  
34 data is not appropriate, as the short time period available is likely to be affected by the temporal  
35 evolution of the wind industry (for example, improvements in reliability) and is therefore unlikely to  
36 capture the full effects of spatial variability and the locations of generation capacity. Sinden (2007)  
37 presented one of the earliest generation potential models for the UK using 10m wind speeds  
38 measured at 66 meteorological stations over a climatologically representative 34-year period.  
39 Having scaled surface wind speeds to hub height and converted these to potential power output  
40 using a turbine power curve, the author examined a number of characteristics of the hypothetical  
41 generation represented by these wind conditions. Pöyry (2009) followed this with a study of wind  
42 power variability for the UK and Ireland based on wind speeds measured at 36 meteorological  
43 station locations over a relatively short period of only 8 years, and using Monte-Carlo techniques to  
44 resample the data, created future scenarios with different installed capacities. Aguirre et al. (2009)  
45 used records for 7 years from 116 meteorological stations grouped into 16 regions of Great Britain  
46 (GB) to develop an estimated time series of aggregate wind power capacity factor. The influence of  
47 each region was weighted by its installed wind power capacity, and the model calibrated to match  
48 reported aggregate capacity factors. Sturt & Strbac (2013) expanded upon this dataset by using it to  
49 develop statistical time series models to create future scenarios, including adjustments to correct for  
50 different wind characteristics found offshore.

51 These studies, whilst valuable, did not account for the fact that wind measurement stations are not  
52 necessarily located close to or in similar topographical situations to the existing wind farms, and it is  
53 therefore possible that the actual spatial effects of wind variability may not be fully represented. In  
54 Ireland, the locations of the national meteorological measurement stations do not coincide  
55 particularly well with locations of wind generation (Figure 1). Kubik et al. (2011) showed that even  
56 using nearby meteorological measurement stations to estimate wind farm generation, whilst  
57 reasonably reflecting the long-term energy production, produces errors in the hourly power output.  
58 These authors discuss how this result has implications for using such methods to study temporally  
59 sensitive parts of the energy system, such as power flow and system balancing.

60 The process of meteorological reanalysis involves running numerical weather prediction models in  
61 'hindcast' mode (i.e. for a historical period) whilst assimilating actual observations throughout the  
62 period to constrain the model and produce homogenous data that reflect the actual conditions.  
63 Typically, such datasets cover periods of 30-40 years (e.g. Rienecker *et al.* (2011)), with some  
64 covering over 100 years (e.g. Compo *et al.* (2011)). Long-term reanalyses products have recently  
65 been proven as a promising alternative to meteorological observations in reproducing both the long-  
66 and short-term characteristics of aggregate regional and national generation patterns in the UK and  
67 Sweden (Cannon et al., 2015; Kubik et al., 2013; OFGEM, 2013; Olauson et al., 2015), and even show  
68 reasonable performance at wind-farm level (Kubik et al., 2013; Staffell et al., 2014). A useful  
69 summary of the existing comparisons in the literature of reanalysis-based wind speed data against  
70 measured data is provided in Sharp et al. (2015). The authors found that the Climate Forecast  
71 System Reanalysis (CFSR) dataset could provide a representative view of UK wind climate, but also  
72 identified a lower skill at higher elevations. Aigner & Gjengedal (2011) discuss the differences  
73 between reanalysis- and measurement-based generation models for Germany and Denmark, with  
74 success of measurement-based models being related to the density of measurement stations  
75 available and topography.



76

77 *Figure 1 Locations of wind farms and met stations in Ireland*

78 There is further potential in using downscaled reanalysis data, which should capture more of the  
 79 local variations in wind climate (Cradden et al., 2014). This was demonstrated, for example, in  
 80 Harrison et al. (2015) and Dunbar et al. (2015) where the Weather Research and Forecasting (WRF)  
 81 mesoscale model driven by the National Centers for Environmental Prediction/National Center for  
 82 Atmospheric Research (NCEP/NCAR) reanalysis was used to calculate capacity credit for wind power  
 83 and arbitrage revenue from storage, respectively. The disadvantage of such high resolution datasets  
 84 is that, aside from the resources required to produce them, they require significantly more storage  
 85 and computational time when used to derive a generation model.

86 Based on comparison against real production data in the shorter term, reanalysis-based models,  
 87 whether downscaled or not, offer the potential to examine the impact of longer-term climate  
 88 variability on energy systems with a high contribution from wind generation. The World  
 89 Meteorological Organisation (WMO) define 30 years as the period required to represent a ‘climate  
 90 normal’, i.e. typical long-term average conditions (World Meteorological Organization, 2011),  
 91 although some evidence would suggest that such periods do not capture the entire potential range  
 92 of variability, e.g. Bett *et al.* (2013). The full impacts of spatial variability, including future planned  
 93 generation sites, can also be studied using reanalysis models as they cover wide areas with equal  
 94 density and temporal coherence. Additionally, such models can help to identify and analyse longer-  
 95 term and wider-ranging climatic patterns influencing wind generation. For example, this approach  
 96 would offer an alternative to the statistical wind data generation techniques used to examine the  
 97 effects of the NAO in Brayshaw et al. (2011), Curtis et al. (2016) and Ely et al. (2013).

98 **1.1. Objectives**

99 Ireland is a relatively small but topographically complex country, and the wind industry has seen very  
 100 rapid growth in recent years, from just over 100 MW of installed capacity at the end of 2001 to  
 101 around 2200 MW by the end of 2014. Pöyry (2009) simulated Irish wind power generation but the  
 102 study was based on meteorological stations unrelated to generator locations. Grünewald, McKenna,  
 103 & Thomson (2015) used wind speeds at 10m above ground level (a.g.l.) from a reanalysis dataset to  
 104 model power production for the whole of Ireland for the short period from 2009-2012, but  
 105 employed a relatively simplistic height transformation and power conversion process, and  
 106 generalised the locations by county. It is useful to determine whether a detailed reanalysis-based  
 107 generation model can be used to provide an accurate representation of the aggregate wind power  
 108 output for a region of this size over a long period of time.

109 In this study a detailed wind generation potential model is first developed for the Republic of Ireland  
110 for a 14 year period (2001-2014) based on MERRA reanalysis data (Rienecker et al., 2011). Wind  
111 farm locations, specifications and connection dates are input to the model and the output verified  
112 by comparison with the actual production as reported by the grid operator, EirGrid (EirGrid, 2015b).  
113 For a sample year within this period (2006), the output of the model based on reanalysis data is  
114 compared with output from the same model driven by two very high resolution wind speed  
115 datasets, which might be expected better to capture the complexities of the local wind climate.

116 Due to their ability to produce long time series, reanalysis-based models are well suited to  
117 applications involving understanding the impact of large-scale climate features on regional wind  
118 generation patterns. Having successfully verified for the 14 year period, the model is then used to  
119 generate a hypothetical 34-year time series of aggregate wind generation for Ireland based on the  
120 actual installed wind capacity as of October 2015. Aggregate generation output is then examined in  
121 relation to some atmospheric patterns, the NAO and the EA, to ascertain the influence of these  
122 features on generation characteristics.

## 123 2. Simulating and verifying Irish wind generation 2001-2014

124 The model estimates hourly aggregate wind power output for the Republic of Ireland from 2001-  
125 2014, based on the location, capacity, date of generation commencement, and hub heights of  
126 turbines at wind farms around the country. This is compared with a dataset provided by the system  
127 operator, EirGrid, consisting of hourly actual wind power production values for the same time  
128 period.

### 129 2.1. Wind farm data

130 The name, capacity and connection date of each wind farm was provided by the grid operators  
131 (EirGrid (2015a) and ESB Networks (2015)) correct as of October 2015. Further wind farm  
132 specifications were obtained from the Irish Wind Energy Association (IWEA) and the Sustainable  
133 Energy Authority Ireland (SEAI). The location information was gathered manually using online  
134 mapping services to identify those farms in existence before the last update of the satellite images  
135 (c. 2012/2013). For those developed after this time, the name of the wind farm locality was used to  
136 estimate its geographic coordinates within +/-10km. Given the use of relatively low-resolution  
137 (~50km) reanalysis wind speed data as input, location uncertainties can be considered to be  
138 negligible.

### 139 2.2. Wind data

140 The primary source of wind data used for this study is the MERRA reanalysis dataset (Rienecker et  
141 al., 2011), as used by Cannon et al., (2015), OFGEM (2013) and Staffell & Green (2014). MERRA  
142 includes hourly surface wind fields on a 0.5 x 0.667 degrees latitude/longitude grid, which equates to  
143 a spatial resolution of around 50 km x 50 km, and was chosen in preference to other large-scale  
144 reanalyses products due to its provision of wind fields at different heights above ground level. To  
145 establish wind speeds at turbine hub heights, we followed the method of Cannon et al. (2015). For  
146 each wind farm location, the wind speeds at 2, 10 and 50m above ground level (a.g.l) are  
147 interpolated from the surrounding grid cells using bilinear splines to the required latitude/longitude.  
148 A logarithmic fit is found for the values at the three heights at the interpolation point, and  
149 extrapolated to the required hub height, typically 60-80m.

150 For comparison, the model has been re-run for a single year (2006) using two alternative wind  
151 resource datasets. Firstly, UK Meteorological Office (UKMO) Virtual Met Mast (VMM) data were  
152 provided by the SEAI (Standen et al., 2013). These 2006 data consist of hourly time series on a 1 km  
153 grid (bi-linearly interpolated from the original 4 km model resolution) at 20, 30, 40, 50, 75, 100, 125

154 and 150m a.g.l. The VMM model uses a log-linear fit assumption from a baseline height to establish  
 155 the winds at these levels, so the fit equation is approximated from the data and is used to  
 156 interpolate to turbine hub height.

157 The second high-resolution dataset is that used by Dunbar et al. (2015) and Harrison et al. (2015),  
 158 developed at the University of Edinburgh. These data, derived from the WRF mesoscale model, are  
 159 on a regular 3km grid covering the UK and Ireland. The model outputs were provided for the year  
 160 2006 at 10, 80 and 100m above ground level. As the model itself does not assume a particular  
 161 vertical profile, a logarithmic fit was used to provide an interpolation function for turbine heights  
 162 between these values (no wind farm hub height was above 100m).

### 163 2.3. Power calculation

164 To convert turbine hub height wind speeds to wind power output, a ‘power curve’ is used.

165 For individual turbines, power curves are often provided by the manufacturer based on measured  
 166 output data for given wind speeds. For a wind farm, the curve representing the aggregate output of  
 167 a number of turbines will be slightly different (Hayes et al., 2011). To represent an entire national  
 168 fleet, further adjustments may be required. Cannon et al. (2015) present a power curve based on a  
 169 single turbine, but modified to fit GB aggregate output, and this is applied here. Other modifications  
 170 can be introduced, particularly with respect to the cut-out region of the function (OFGEM, 2013).  
 171 Selected results from model runs using alternative power curves are presented in the supplementary  
 172 material.

## 173 3. Model verification

### 174 3.1. Comparison of general characteristics

175 Over the 14 year comparison period, the basic summary parameters based on hourly production in  
 176 MW for the model output and actual production data are shown in Table 1.

177 *Table 1 Basic statistics from actual and model data, all values in MW, except for coefficient of variation*

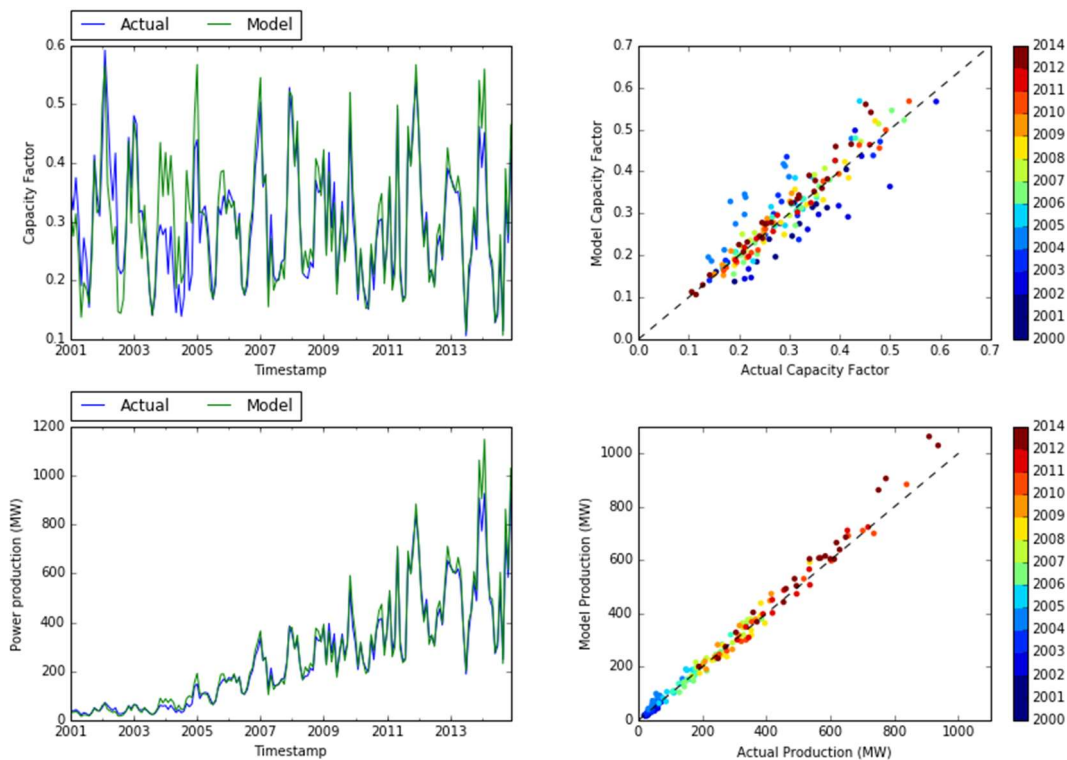
Year	Mean		Maximum		Standard deviation		Coefficient of variation	
	Actual	Model	Actual	Model	Actual	Model	Actual	Model
2001	35	31	107	110	30	27	0.86	0.88
2002	46	39	119	121	33	31	0.72	0.80
2003	45	48	130	184	34	40	0.76	0.82
2004	57	79	278	295	49	65	0.86	0.82
2005	118	126	452	437	91	102	0.78	0.81
2006	178	185	643	606	142	150	0.80	0.81
2007	215	208	708	650	172	173	0.80	0.83
2008	262	278	888	835	197	207	0.75	0.75
2009	329	328	1050	1102	245	252	0.74	0.77
2010	297	311	1222	1230	250	273	0.84	0.88
2011	486	484	1468	1405	377	390	0.78	0.80
2012	467	473	1492	1505	336	365	0.72	0.77
2013	530	562	1760	1774	397	456	0.75	0.81
2014	577	639	1813	1975	455	535	0.79	0.84
<b>Overall</b>	<b>260</b>	<b>271</b>	<b>1813</b>	<b>1975</b>	<b>308</b>	<b>335</b>	<b>1.19</b>	<b>1.24</b>

178

179 The model successfully captures the basic production characteristics. There is evidence of  
 180 underestimation of the mean and standard deviation of production in 2001/2002 where installed  
 181 capacity was low, but the model overestimates the annual maxima until 2005.

182 Figure 2 compares the modelled monthly mean capacity factors and production values (MW) with  
 183 the actual values. The capacity factor is effectively the capacity-normalised power production,  
 184 allowing comparison of each year on an equal basis. After 2005, the monthly mean capacity factors  
 185 are well reproduced by the model (Figure 2, upper panel), with overestimation in a few months. The  
 186 correlation is strong, with the largest outliers in the early years (blue points in the upper right panel),  
 187 indicating that the model is capable of representing the monthly average aggregate patterns in wind  
 188 generation, but perhaps only after a certain minimum installed capacity has been attained. As only a  
 189 small number of sites are included in these early years, biases resulting from the low spatial  
 190 resolution of the MERRA wind speed data will be particularly obvious with this low degree of  
 191 aggregation.

192 Analysis of the monthly production values provides further insight (Figure 2, lower panels). In the  
 193 early years, when the power output is relatively small, the corresponding absolute errors in these  
 194 years are also small compared with the later years. There is a growing tendency to overestimate  
 195 production in some recent years (Figure 2, red and orange points in lower right panel), which may be  
 196 indicative of curtailment, i.e. production is deliberately reduced by the operator. This operational  
 197 strategy for managing large power input to networks has only become necessary in recent years as  
 198 capacity has increased significantly.

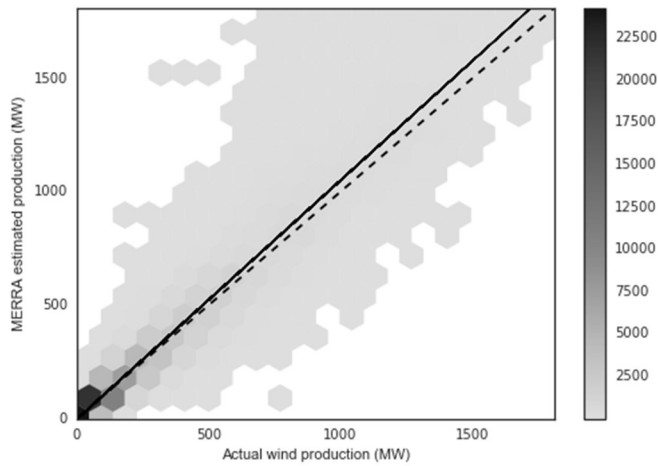


199

200

201 *Figure 2 Monthly mean capacity factor (upper) and production values (lower) for the model calibration period (2001-2014).*  
 202 *The correlation coefficient is 0.91 for monthly capacity factors and 0.99 for production.*

203 A density plot of the actual and modelled hourly production values highlights a tendency for  
 204 overestimation in the model, with the best fit line (heavily influenced by the higher number of  
 205 occurrences in the 0-250 MW range) being slightly steeper than the ideal  $y=x$  line. Seasonal  
 206 differences between model and actual capacity factor distributions are shown in the supplementary  
 207 material.



208

209 *Figure 3 Density plot of modelled vs. actual hourly production. Dashed line is the y=x line, solid line is the best fit line.*

210 **3.2. Analysis of model error**

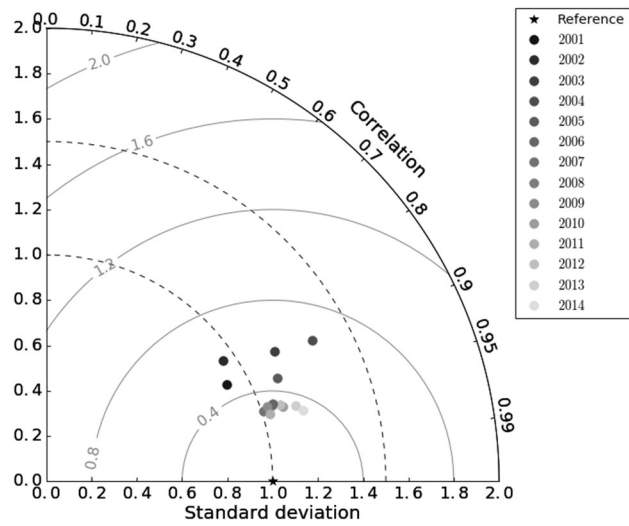
211 The error statistics for each year are shown in Table 2, with the bias and RMSE given as percentages  
 212 of the installed capacity (as per Kubik et al. (2011), Olauson & Bergkvist (2015)).

213 *Table 2 Error statistics for each year (MERRA)*

<i>Year</i>	<i>Correlation</i>	<i>Bias</i>	<i>RMSE</i>	<i>Scatter Index</i>
2001	0.88	3.46%	12.32%	0.42
2002	0.83	5.37%	16.29%	0.44
2003	0.87	-1.33%	11.73%	0.44
2004	0.88	-9.19%	15.74%	0.68
2005	0.91	-1.93%	10.76%	0.36
2006	0.95	-0.89%	8.24%	0.28
2007	0.95	0.93%	7.76%	0.25
2008	0.95	-1.86%	8.05%	0.26
2009	0.95	0.33%	7.84%	0.25
2010	0.95	-1.09%	6.40%	0.28
2011	0.96	0.10%	7.66%	0.23
2012	0.95	-0.35%	7.07%	0.24
2013	0.96	-1.71%	7.79%	0.27
2014	0.96	-2.94%	7.98%	0.29
<b>Overall</b>	<b>0.97</b>	<b>-0.79%</b>	<b>10.17%</b>	<b>0.33</b>

214

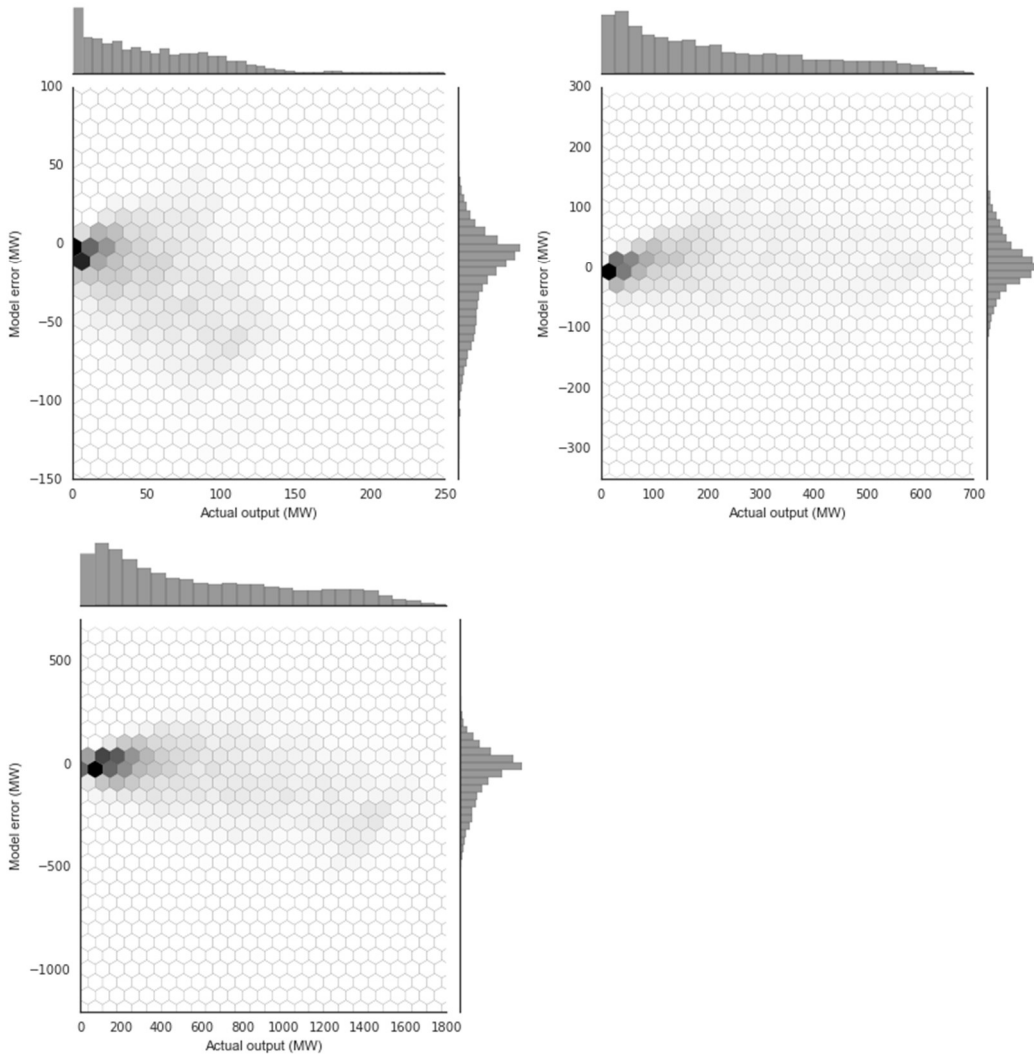
215 These statistics can be visualised using a normalised Taylor diagram (Figure 4). A detailed description  
 216 of the diagram construction is given in Taylor (2005). Fundamentally, the closer the points to the  
 217 'reference' point, the better the model. The diagram visually reinforces the case that recent years  
 218 are better represented by the model than the earlier years of the verification period.



219

220  
221  
222

Figure 4 Taylor diagram - points for each year are plotted according to their relative standard deviation compared to the reference data (i.e. normalised, so the reference data has a standard deviation of 1) and the correlation between the time-series. Geometrically, the distance between the yearly points and the reference point is then the RMSE.



223

224

225

Figure 5 Model error vs. production for 2004 (top left), 2007 (top right) and 2014 (bottom left)

226 Scatter plots of the hourly errors (defined as 'Actual – Model') compared with the actual production  
227 for three of the years, 2004 (worst), 2007 (best) and 2014 (most recent), are shown in Figure 5. The  
228 model overestimates production throughout most of the analysis period, so that the error has a  
229 tendency to be negative. The year 2007, which performs well according to the previously described  
230 metrics but actually has a small positive bias, shows the most normal distribution of errors  
231 throughout the range of actual power production figures. In 2004 and 2014, the negative error  
232 increases with increasing generation. In 2004, this tendency may be due to biases in the wind speeds  
233 or lower than expected availability, but in 2014 is more likely to be related to curtailment.

### 234 3.3. Operational considerations

235 The power curve, as mentioned previously, has been created to be representative of national  
236 aggregate output for a given wind speed. Due to its empirical nature, it includes some operational  
237 factors that are present in the data used to derive it. No additional adjustments have been made to  
238 the model to account for specific operational practices such as maintenance (planned or  
239 unplanned), nor does the model consider performance issues resulting from early life start-up issues  
240 or long-term degradation in performance. The lack of operational considerations should lead to a  
241 tendency for the model to overestimate production.

242 At the beginning of the verification period, aside from the errors arising from the small degree of  
243 aggregation combined with low resolution wind speeds, there may be contributions from start-up  
244 date inconsistencies and unknown operational or reliability factors. From around the second half of  
245 2003 until the end of 2005, the model produces the expected overestimates in many months. It is  
246 after this period, when total installed capacity reaches 500 MW, that the model estimates appear to  
247 be most accurate. Towards the latter end of the verification period, there is evidence that the  
248 capacity factor is being overestimated at the highest values. A probable operational contributor to  
249 these errors in recent years relates to the curtailment of wind generation by the network operator.  
250 Reasons for curtailment<sup>1</sup> are given in detail for the year 2014 in O'Sullivan et al. (2014). These  
251 include maintaining system stability, voltage control, and application of a feasible limit for absorbing  
252 non-synchronous power. Locally, wind output can also be curtailed due to local network faults and  
253 constraints.

254 An approximate time series of curtailed power was provided by the system operator, EirGrid, and  
255 made available for this study via the SEAI for 2012-2014. Reducing the model output by the  
256 percentage of power curtailed improves the RMSE by 0.75% (2012), 1.12% (2013) and 1.21% (2014),  
257 and very slightly improves the hourly correlations. This indicates that the presence of curtailment in  
258 the production data is a likely contributor to the additional model error in these years.

### 259 3.4. Using different wind resource data

260 Two sets of wind speed data with a significantly higher spatial resolution than MERRA were used to  
261 generate a year (2006) of aggregate production data. An identical power curve and set of wind farm  
262 information have been used. Due to their improved spatial resolution, both datasets might be  
263 expected to be more representative of the wind conditions at any one wind farm.

#### 264 3.4.1. Wind speeds at 10m

265 It is difficult to validate the wind speeds from the datasets at turbine hub-height due to lack of wind  
266 speed measurements at these heights. Analysis of the 10m wind speeds from the three reanalyses  
267 compared to a set of 10m measured wind speeds in Ireland for the year 2006 is presented in the

---

<sup>1</sup> Curtailment is termed by the network operator as 'dispatch-down'; 'curtailment' is used to refer to a specific reason for dispatch-down

268 supplementary material. The results for MERRA are consistent with Cannon et al. (2015), with the  
 269 low wind speeds tending to be higher than the measured, whilst at high measured speeds, MERRA  
 270 appears to underestimate. Cannon et al. (2015) also found that changes in wind speeds over small  
 271 time intervals were underestimated. In comparison with measured 10m wind speeds, the higher  
 272 resolution WRF data performed better than MERRA, having higher correlations with hourly time  
 273 series, and lower bias and RMSE. The VMM data have lower correlation with measurements, but  
 274 have been extrapolated down to 10m from model output at higher levels so this may not provide a  
 275 fair comparison.

276 Higher resolution models will be more sensitive to uncertainty in wind farm locations – the  
 277 resolution of the alternative data is 1-3km, rather than ~50km with MERRA. In areas of complex  
 278 terrain, this may lead to larger errors in the production estimates for individual wind farms.

### 279 *3.4.2. Comparison of alternative models*

280 A comparison of the data characteristics and error statistics for the one year of high-resolution  
 281 datasets with those from the MERRA-based output is presented in Table 3. The correlation of the  
 282 VMM data with actual output is lower than that achieved when the model is run using MERRA, and  
 283 the scatter index and RMSE values from the VMM data are higher. The overall bias, however, is  
 284 lowest, with the mean and standard deviation closer to the original data. In comparison, the WRF  
 285 output has a similarly strong correlation with the actual power-generation data as the MERRA  
 286 version. The mean is higher than the actual, close to the MERRA value, and the output has a similar  
 287 bias. The WRF RMSE is the lowest. All models underestimate the maximum output to a similar  
 288 degree.

289 For the year of comparison, Figure 6 shows the monthly average capacity factors and power  
 290 production for the three models compared with the average recorded production for each month.  
 291 All three models are most successful in spring (March, April, May), whilst for September-December,  
 292 the VMM model is best. The WRF-based data tend to overestimate production in winter, and  
 293 underestimate in summer.

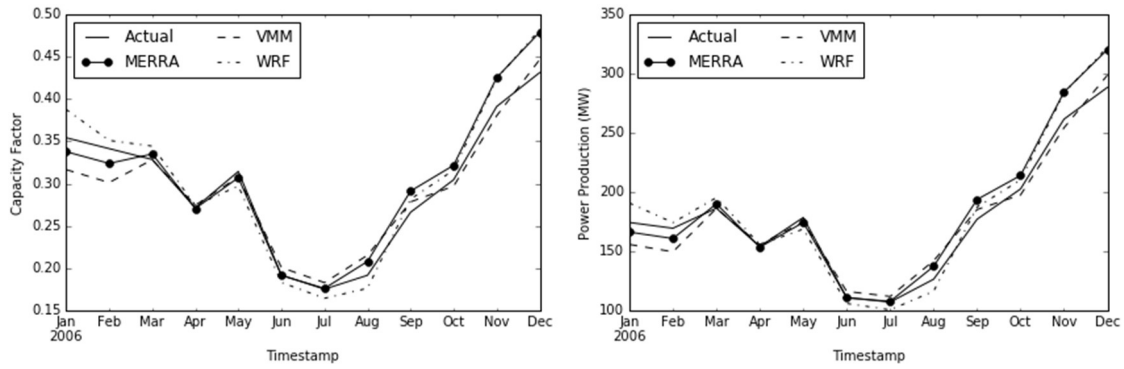
294 *Table 3 General characteristics of the model output and error statistics*

	<i>Mean</i>	<i>Maximum</i>	<i>Standard deviation</i>	<i>Coefficient of Variation</i>
<i>Actual</i>	178	643	142	0.80
<i>MERRA</i>	185	606	150	0.81
<i>VMM</i>	177	605	143	0.81
<i>WRF</i>	184	607	143	0.78

	<i>Correlation</i>	<i>Bias</i>	<i>RMSE</i>	<i>Scatter Index</i>
<i>MERRA</i>	0.95	-0.89%	8.24%	0.28
<i>VMM</i>	0.91	0.24%	10.36%	0.35
<i>WRF</i>	0.95	-1.00%	7.3%	0.25

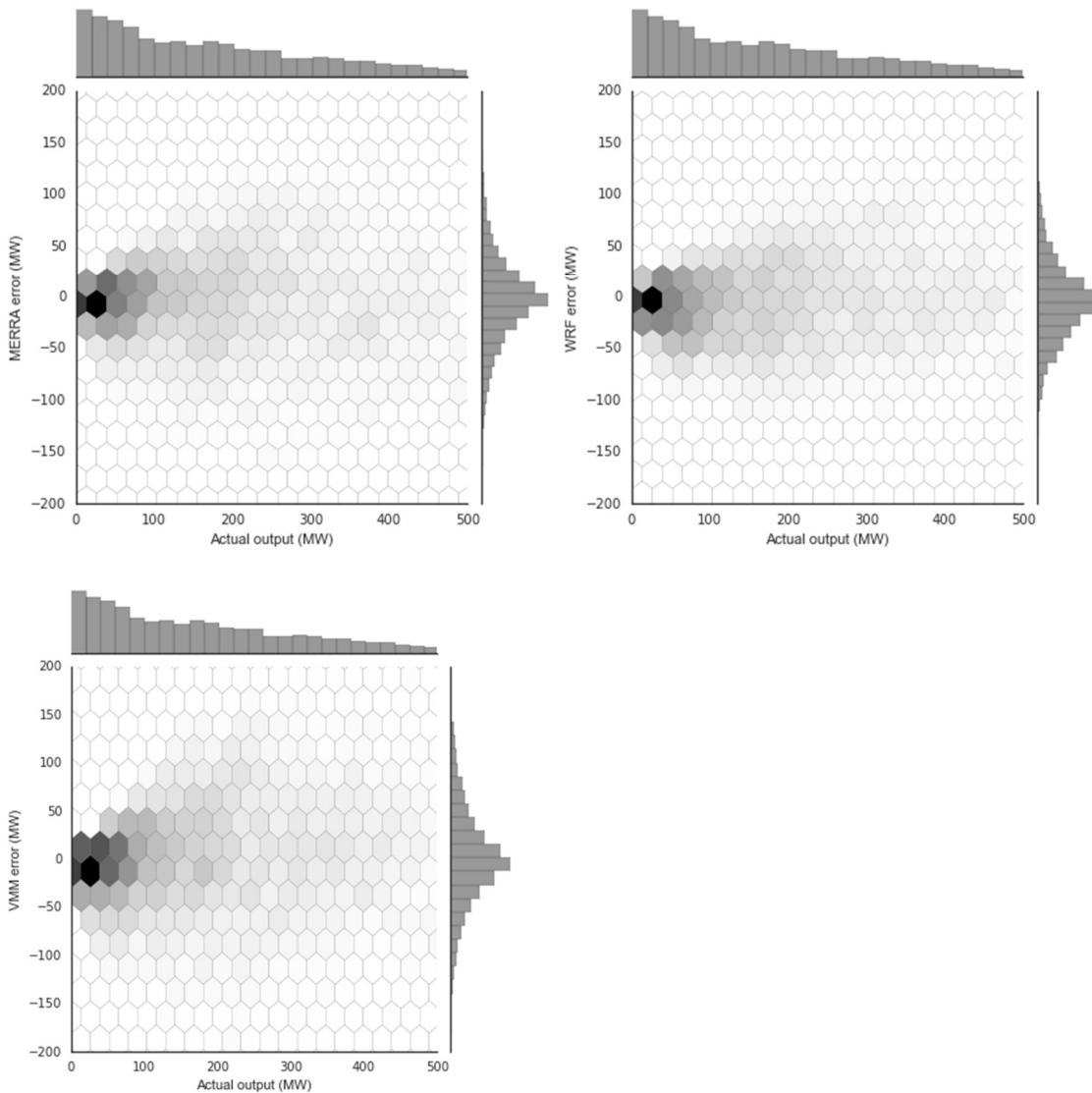
296



297

298 *Figure 6 2006 Monthly capacity factor (left) and power production (MW, right) from the three models compared to actual*

299 Considering the scatter plots of model error vs. actual production (Figure 7) the model errors all tend  
 300 to approximate a 'normal' distribution. The distribution from the VMM-driven model shows the  
 301 largest spread in the errors, with the MERRA and WRF versions slightly narrower in range.



302

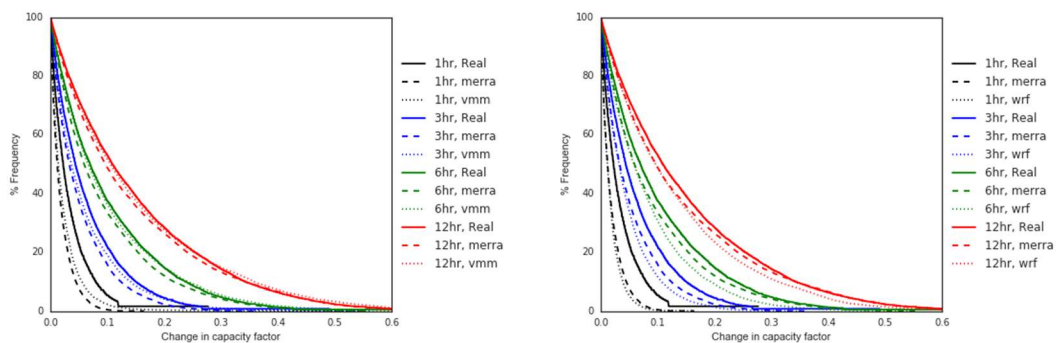
303

304 *Figure 7 Comparison of model errors for 2006*

305 *3.4.3. Ramping events*

306 Changes in capacity factors on the system hour-by-hour are particularly relevant to network and  
307 power system operations. A ‘ramp’ is defined for each hour,  $t$ , as the difference between capacity  
308 factor at time,  $t$ , and the capacity factor at time  $t + horizon$ . The cumulative frequency of ramps at a  
309 range of time horizons is shown in Figure 8. Similarly to Cannon et al. (2015), these plots represent  
310 the percentage of hours which precede a change in capacity factor (positive or negative) of at least a  
311 given size at the specified time horizons. The observed distributions are shown by solid lines, and the  
312 model distributions by dashed lines. For example, at a time horizon of 3 hours, the ramp that follows  
313 10% of hours is actually around +/-14%, whilst the MERRA-driven model predicts this to be around  
314 +/-11%. Generally, at horizons of 1-3 hours for a given percentage of hours, the model produces  
315 ramps of a smaller magnitude than observed, but at 6 hours and beyond, the model ramping more  
316 closely matches reality.

317 The VMM data (Figure 8, left) offer an improvement in representing ramping events at shorter time  
318 horizons of 1, 3 and 6 hours, with the curve on the graph being slightly closer to that of the actual  
319 data compared with the MERRA curve. At 12 hours, both appear to have similar levels of difference  
320 to the real data. In the case of the model based on WRF (Figure 8, right), at all time horizons it  
321 underestimates the frequency of changes of a given magnitude. No difference was found between  
322 day-time and night-time ramping events.



323

324 *Figure 8 Model ramping compared with Actual. (Left) VMM and MERRA, (Right) WRF and MERRA.*

325 In summary, when used in the generation model, the higher resolution data do not necessarily add  
326 skill to the model in all areas of assessment. While there is some improvement in predicting  
327 generation ramps at short time horizons using the VMM data, the correlation on an hourly basis  
328 using these data over the whole year is lower. The model output using WRF is comparable to that  
329 based on MERRA data, but it does not appear to capture the aggregate power ramping at short  
330 timescales. The end-use of the model output should be considered, therefore, when making a  
331 choice.

332 *4. Application of model: Large-scale climate features and wind generation*

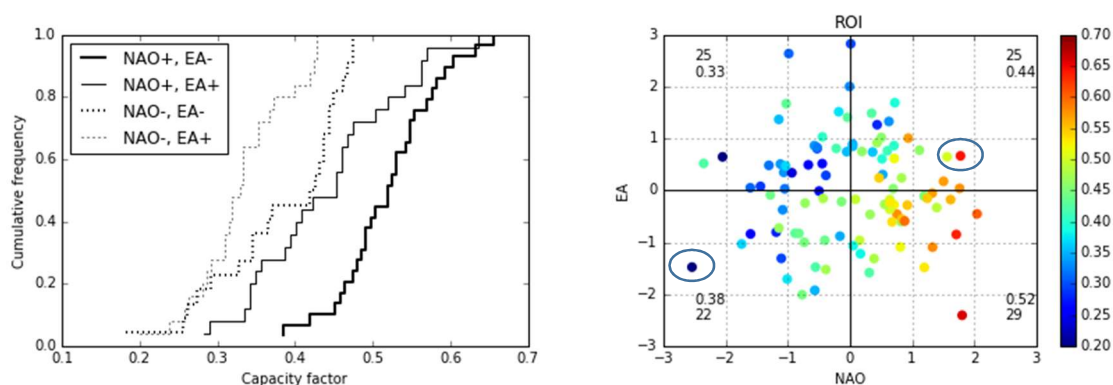
333 The role of the North Atlantic Oscillation (NAO) has received some attention with regard to wind  
334 resources in recent years (e.g, Brayshaw et al. (2011); Ely et al. (2013)). Both studies used  
335 representations of local wind generation derived from a small number of meteorological  
336 measurements to establish correlations between hypothetical winter wind power output and the  
337 NAO index. Here, we use the MERRA-based wind generation model to consider the impact of the  
338 NAO on 34 years of simulated aggregate power output for the Republic of Ireland in winter,  
339 assuming the installed capacity as of 2014. Like most studies considering the NAO, the focus here is  
340 on the winter months of December, January and February, where the influence of the NAO on

341 surface weather variables is strongest and most consistent (e.g. (Hurrell, 1995). The capacity factors  
 342 for all the December, January and February months have been extracted from the years 1980-2013  
 343 and compared with an NAO index for those months. A second index, the East Atlantic pattern (EA)  
 344 that is captured by the 2<sup>nd</sup> principal component of sea-level atmospheric pressure variability in the  
 345 region has been shown to modulate the influence of the NAO on winter weather conditions,  
 346 including wind speeds, around Europe (Laia Comas-Bru et al., 2014), and is considered here  
 347 alongside the NAO.<sup>2</sup> The NAO and EA indices used here are taken from Zubiate et al. (2016) and are  
 348 based on a separate reanalysis dataset, ERA-Interim. It was shown in Comas-Bru *et al.* (2016), that  
 349 the differences between NAO and EA indices from two different reanalyses products are small and  
 350 here, as with Ely et al. (2013), it will not impact noticeably on the results of the analysis.

#### 351 4.1. Monthly mean capacity factors

352 Figure 9 presents the relationship between the aggregate monthly mean capacity factor for the  
 353 Republic of Ireland and the NAO and EA indices. The left-hand panel shows the empirical cumulative  
 354 distribution for monthly mean capacity factor for the four sets of NAO and EA conditions. A  
 355 Kolmogorov-Smirnoff two-sample test of significance is used to determine if the empirical  
 356 probability density functions of the monthly mean capacity factors are significantly different in the  
 357 EA+ or EA- state. The results suggest that the differences are significant when the NAO is both  
 358 positive (p-value = 0.0009) and negative (p-value = 0.009), i.e. the likelihood of the differences being  
 359 due to random error are less than 1% in both cases. It can be concluded that in those months where  
 360 the NAO is negative and lower wind production is expected, that a concurrently negative EA may  
 361 partly offset the effects of this.

362 The right hand panel of Figure 9 shows the individual capacity factors and the corresponding  
 363 NAO/EA values, displaying the outliers more clearly including February 2010 when capacity factor  
 364 was modelled at its minimum, 18%, and yet the EA was quite strongly negative. There is a  
 365 corresponding opposite extreme case, January 1983, when the simulated capacity factor was 64%,  
 366 but the EA was positive. Whilst the combinations of the two patterns do have an apparently  
 367 significant effect on the probability distributions of capacity factors associated with each scenario,  
 368 care is required when looking at individual results.



369

370 *Figure 9 Influence of the NAO and EA on mean monthly aggregate wind generation capacity factors for December, January*  
 371 *and February 1980-2013 in the Republic of Ireland. Left panel – cumulative frequency of capacity factors for each NAO/EA*  
 372 *combination. Right panel – Individual monthly NAO/EA combinations, colour scale is the corresponding capacity factor.*  
 373 *(Number of months represented by the number in the twenties, and mean capacity factor by the lower number.)*

<sup>2</sup> It should be noted that the EA patterns discussed here follow the sign convention presented in (Laia Comas-Bru et al., 2014). Some other studies use the opposite.

374 **4.2. Ramping events**

375 The occurrence of large ramp events is one of the most problematic issues for network operators to  
 376 manage, and it is possible that the frequency of such events is different depending on the prevailing  
 377 NAO/EA combination. It was shown in an earlier section that the model is less successful at  
 378 reproducing ramps at time horizons of around 1-3 hours, but improves in accuracy at longer time  
 379 horizons, so only 6 hours and greater will be considered here.

380 The data are partitioned into four, depending on the NAO/EA combination for the winter month  
 381 (DJF) in which each hour occurs, and the number of ramp events exceeding a specific size is  
 382 calculated. The number of hours which precede these ramps is then converted to a percentage of  
 383 the total hours in that NAO/EA state. The results are shown for ramps of greater than 20% at a 6  
 384 hour time horizon.

385 *Table 4 Ramping events under NAO/EA combinations*

State	% of hours preceding a ramp >20% at 6-hour horizon
NAO+	21%
NAO-	14%
NAO+ / EA+	18%
NAO+ / EA-	23%
NAO- / EA+	12%
NAO- / EA-	17%

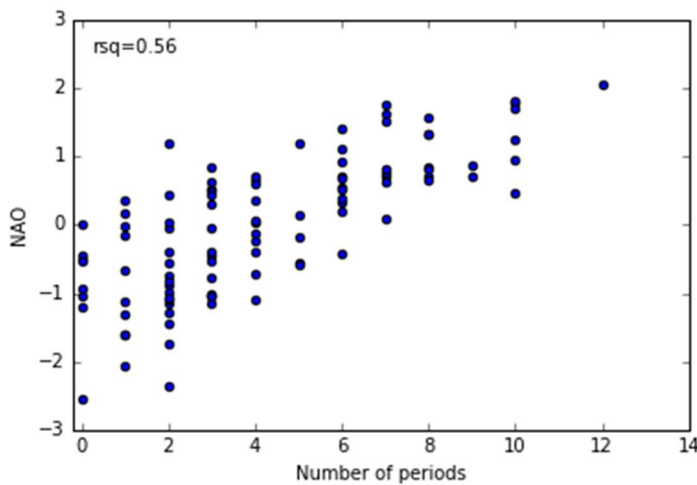
386

387 The percentage occurrence of the specified ramps at 6 hours for NAO+ and NAO- conditions are 21%  
 388 and 14% of hours respectively. A simultaneous EA- state increases the occurrence of these ramps  
 389 compared to EA+ under both NAO states. This corresponds to the general increase in capacity  
 390 factors under the same conditions. No difference was found between ramping during night or day  
 391 time.

392 **4.3. Persistence**

393 A further feature of the large-scale atmospheric patterns worth considering is their influence on  
 394 persistence. From the cumulative distribution, the 20<sup>th</sup> percentile aggregate capacity factor is around  
 395 13%, and the 80<sup>th</sup> percentile is around 74%. Figure 10 shows the number of periods when the  
 396 capacity factor remained above 74% for more than 12 hours compared to the NAO, for each winter  
 397 month in the 34-year period. There is a positive relationship ( $r$ -squared = 0.56), indicating that the  
 398 more positive the NAO, the more likely there will be persistent periods of high aggregate output. The  
 399 same relationship does not hold so strongly in the opposite case, i.e. there is only a weak

400 relationship between persistent low-wind conditions and the NAO index ( $r$ -squared = 0.29). The EA  
401 does not appear to have a discernible influence on persistence.



402

403 *Figure 10 Monthly mean winter NAO vs. number of periods per month over 12 hours long where the capacity factor is above*  
404 *74%. Each point represents an individual December, January or February.*

## 405 5. Conclusions

406 This study presents a comparison of actual wind power generation output in Ireland with modelled  
407 generation using reanalysis wind speed data over a period of 14 years. It includes years when the  
408 wind industry was relatively young with a small number of wind farms, as well as more recent years  
409 with a well-established operational system. In general, based on comparison of basic statistics and  
410 error analysis, the model output driven by MERRA reanalysis data compares well with the real  
411 production data. The time series are strongly correlated and the errors approach a normal  
412 distribution. The model improves as the industry matures and installed capacity increases. A useful  
413 extension to the model would include development of a representation of operational  
414 characteristics, particularly curtailment, to be applied to the output to reproduce realistic scenarios  
415 for the most recent years.

416 In terms of capturing characteristics of generation that are of interest for energy systems analysis,  
417 the model represents the statistics such as monthly mean capacity factor well in most cases, and the  
418 distributions of hourly power output are close to the actual data. Representation of  
419 variability/ramping needs careful consideration and may be susceptible to error at small time  
420 horizons. Different input resource data has been shown potentially to improve the representation,  
421 but careful analysis is necessary to ensure the limitations are fully understood. An alternative would  
422 be to apply an additional higher frequency signal on top of the MERRA output to represent this  
423 variability statistically.

424 An application of the model in 'simulation mode' has been presented. It demonstrates that, based  
425 on the 2014 installed generation with no additional operational conditions applied, the NAO has a  
426 discernible effect on the distribution of winter mean monthly capacity factor in the Republic of  
427 Ireland, with negative NAO months tending to have lower capacity factors, on average. The impact  
428 of the EA is also significant, with EA- states causing a higher average capacity factor for a given NAO  
429 state. The combined NAO/EA states in which there are larger capacity factors correspond to more  
430 frequent occurrences of large ramps in capacity factor. More positive NAO states also lead to more  
431 frequent episodes with persistently high capacity factor events.

432 The relatively long 34-year time period of analysis based on current wind farm installations provides  
433 some confidence in the distributions of capacity factors for a given NAO/EA state and the likelihood  
434 of encountering large ramping events. Coupled with recent advances in predicting the NAO up to  
435 and including one year in advance (Dunstone et al., 2016; Scaife et al., 2014), this analysis informs  
436 system operators of the likely distribution of wind outputs in upcoming winter months.

### 437 Acknowledgements

438 This publication has emanated from research conducted with the financial support of Science  
439 Foundation Ireland under the SFI Strategic Partnership Programme Grant Number  
440 SFI/15/SPP/E3125. *Lucy Cradden would also like to acknowledge funding from the UCD Energy21*  
441 *program, co-financed through the Marie Skłodowska-Curie FP7-PEOPLE-2013-COFUND program.*  
442 EirGrid and ESB are gratefully acknowledged for the provision of wind farm details and EirGrid for  
443 production data. The authors would also like to thank Dr. David Brayshaw at the University of  
444 Reading for sharing the original model code, the SEAI for advice and provision of data, and Prof.  
445 Gareth Harrison at the University of Edinburgh for the WRF model output.

### 446 References

- 447 Aguirre, P. E. O., Dent, C., Harrison, G., & Bialek, J. W. (2009). Realistic calculation of wind generation  
448 capacity credits. *Cigre*, 1–8.
- 449 Aigner, T., & Gjengedal, T. (2011). Modelling Wind Power Production Based on Numerical Prediction  
450 Models and Wind Speed Measurements. *17Th Power Systems Computation Conference*.
- 451 Bett, P. E., Thornton, H. E., & Clark, R. T. (2013). European wind variability over 140 yr. *Advances in*  
452 *Science and Research*, 10(12th EMS Annual Meeting and 9th European Conference on Applied  
453 Climatology (ECAC) 2012), 51–58. <http://doi.org/10.5194/asr-10-51-2013>
- 454 Brayshaw, D. J., Troccoli, A., Fordham, R., & Methven, J. (2011). The impact of large scale  
455 atmospheric circulation patterns on wind power generation and its potential predictability: A  
456 case study over the UK. *Renewable Energy*, 36(8), 2087–2096.  
457 <http://doi.org/10.1016/j.renene.2011.01.025>
- 458 Cannon, D. J., Brayshaw, D. J., Methven, J., Coker, P. J., & Lenaghan, D. (2015). Using reanalysis data  
459 to quantify extreme wind power generation statistics: A 33 year case study in Great Britain.  
460 *Renewable Energy*, 75, 767–778. <http://doi.org/10.1016/j.renene.2014.10.024>
- 461 Comas-Bru, L., & McDermott, F. (2014). Impacts of the EA and SCA patterns on the European  
462 twentieth century NAO-winter climate relationship. *Quarterly Journal of the Royal*  
463 *Meteorological Society*, 140(679), 354–363. <http://doi.org/10.1002/qj.2158>
- 464 Comas-Bru, L., McDermott, F., & Werner, M. (2016). The effect of the East Atlantic pattern on the  
465 precipitation ??18O-NAO relationship in Europe. *Climate Dynamics*, 47(7), 1–11.  
466 <http://doi.org/10.1007/s00382-015-2950-1>
- 467 Compo, G. P., Whitaker, J. S., Sardeshmukh, P. D., Matsui, N., Allan, R. J., Yin, X., ... Worley, S. J.  
468 (2011). The Twentieth Century Reanalysis Project. *Quarterly Journal of the Royal*  
469 *Meteorological Society*, 137(654), 1–28. <http://doi.org/10.1002/qj.776>
- 470 Cradden, L. C., Restuccia, F., Hawkins, S. L., & Harrison, G. P. (2014). Consideration of wind speed  
471 variability in creating a regional aggregate wind power time series. *Resources*, 3(1), 215–234.  
472 article.
- 473 Curtis, J., Lynch, M., & Zubiate, L. (2016). Carbon dioxide (CO<sub>2</sub>) emissions from electricity: The  
474 influence of the North Atlantic Oscillation. *Applied Energy*, 161, 487–496.

475 <http://doi.org/10.1016/j.apenergy.2015.09.056>

476 Dunbar, A., Cradden, L. C., Harrison, G. P., & Wallace, R. (2015). Impact of wind power on arbitrage  
477 revenue for electricity storage. *IET Generation, Transmission & Distribution*, 10(SEPTEMBER),  
478 798–806. <http://doi.org/10.1049/iet-gtd.2015.0139>

479 Dunstone, N., Smith, D., Scaife, A., Hermanson, L., Eade, R., Robinson, N., ... Knight, J. (2016). Skilful  
480 predictions of the winter North Atlantic Oscillation one year ahead. *Nature Geosci*, 9(11), 809–  
481 814. JOUR. Retrieved from <http://dx.doi.org/10.1038/ngeo2824>

482 EirGrid. (2015a). Connected and contracted generators - Ireland. Retrieved October 1, 2015, from  
483 <http://www.eirgridgroup.com/customer-and-industry/general-customer-information/gate-3/>

484 EirGrid. (2015b). Historical wind generation data. Retrieved October 1, 2015, from  
485 <http://www.eirgridgroup.com/>

486 Ely, C. R., Brayshaw, D. J., Methven, J., Cox, J., & Pearce, O. (2013). Implications of the North Atlantic  
487 Oscillation for a UK–Norway Renewable power system. *Energy Policy*, 62, 1420–1427.  
488 <http://doi.org/10.1016/j.enpol.2013.06.037>

489 ESB Networks. (2015). Connected and contracted generators. Retrieved October 1, 2015, from  
490 [https://www.esb.ie/esbnetworks/en/generator-connections/Connected-Contracted-](https://www.esb.ie/esbnetworks/en/generator-connections/Connected-Contracted-Generators.jsp)  
491 [Generators.jsp](https://www.esb.ie/esbnetworks/en/generator-connections/Connected-Contracted-Generators.jsp)

492 Grünewald, P., McKenna, E., & Thomson, M. (2015). Going with the wind: temporal characteristics of  
493 potential wind curtailment in Ireland in 2020 and opportunities for demand response. *IET*  
494 *Renewable Power Generation*, 9(1), 66–77. <http://doi.org/10.1049/iet-rpg.2013.0320>

495 Harrison, G., Hawkins, S., Eager, D., & Cradden, L. (2015). Capacity Value of Offshore Wind in Great  
496 Britain. *Proceedings of the Institution of Mechanical Engineers, Part O: Journal of Risk and*  
497 *Reliability*. JOUR.

498 Hayes, B. P., Ilie, I., Porpodas, A., Djokic, S. Z., & Chicco, G. (2011). Equivalent power curve model of a  
499 wind farm based on field measurement data. In *PowerTech, 2011 IEEE Trondheim* (pp. 1–7).  
500 inproceedings.

501 Hurrell, J. W. (1995). Decadal Trends in the North Atlantic Oscillation : Regional Temperatures and  
502 Precipitation. *Science*, 269(5224), 676–679.

503 Kubik, M. L., Brayshaw, D. J., Coker, P. J., & Barlow, J. F. (2013). Exploring the role of reanalysis data  
504 in simulating regional wind generation variability over Northern Ireland. *Renewable Energy*,  
505 57(0), 558–561. article. <http://doi.org/http://dx.doi.org/10.1016/j.renene.2013.02.012>

506 Kubik, M. L., Coker, P. J., & Hunt, C. (2011). Using meteorological wind data to estimate turbine  
507 generation output: a sensitivity analysis. In *World Renewable Energy Congress* (pp. 4074–4081).  
508 inproceedings. Retrieved from <http://centaur.reading.ac.uk/28608/>

509 O’Sullivan, J., Rogers, A., Flynn, D., Smith, P., Mullane, A., & O’Malley, M. (2014). Studying the  
510 maximum instantaneous non-synchronous generation in an Island system-frequency stability  
511 challenges in Ireland. *IEEE Transactions on Power Systems*, 29(6), 2943–2951.  
512 <http://doi.org/10.1109/TPWRS.2014.2316974>

513 OFGEM. (2013). Electricity Capacity Assessment Report 2013, 122.

514 Olauson, J., & Bergkvist, M. (2015). Modelling the Swedish wind power production using MERRA  
515 reanalysis data. *Renewable Energy*, 76, 717–725. <http://doi.org/10.1016/j.renene.2014.11.085>

516 Pöyry. (2009). *Impact of intermittency: how wind variability could change the shape of the British*

517            *and Irish electricity markets - Description of Methodology.*

518    Rienecker, M. M., Suarez, M. J., Gelaro, R., Todling, R., Bacmeister, J., Liu, E., ... Woollen, J. (2011).  
519            MERRA: NASA's Modern-Era Retrospective Analysis for Research and Applications. *Journal of*  
520            *Climate*, 24(14), 3624–3648. JOUR. <http://doi.org/10.1175/JCLI-D-11-00015.1>

521    Scaife, a. a., Arribas, a, Blockey, E., Brookshaw, a., Clark, R. T., Dunstone, N., ... Williams, a. (2014).  
522            Skillful long range prediction of European and North American winters. *Geophysical Research*  
523            *Letters*, 5, 2514–2519. <http://doi.org/10.1002/2014GL059637>.Received

524    Sharp, E., Dodds, P., Barrett, M., & Spataru, C. (2015). Evaluating the accuracy of CFSR reanalysis  
525            hourly wind speed forecasts for the UK, using in situ measurements and geographical  
526            information. *Renewable Energy*, 77, 527–538. <http://doi.org/10.1016/j.renene.2014.12.025>

527    Sinden, G. (2007). Characteristics of the UK wind resource: Long-term patterns and relationship to  
528            electricity demand. *Energy Policy*. <http://doi.org/10.1016/j.enpol.2005.10.003>

529    Staffell, I., & Green, R. (2014). How does wind farm performance decline with age? *Renewable*  
530            *Energy*, 66, 775–786. <http://doi.org/10.1016/j.renene.2013.10.041>

531    Standen, J., Wilson, C., & Vosper, S. (2013). Project Report : Remodelling the Irish national onshore  
532            and offshore wind atlas. Retrieved from  
533            [http://www.seai.ie/Renewables/Wind\\_Energy/Wind\\_Maps/2013-Wind-Atlas-Project-](http://www.seai.ie/Renewables/Wind_Energy/Wind_Maps/2013-Wind-Atlas-Project-Reports/VerificationReport_SEAI.PDF)  
534            [Reports/VerificationReport\\_SEAI.PDF](http://www.seai.ie/Renewables/Wind_Energy/Wind_Maps/2013-Wind-Atlas-Project-Reports/VerificationReport_SEAI.PDF)

535    Sturt, A., & Strbac, G. (2013). Times-series modelling for the aggregate Great Britain wind output  
536            circa 2030. *Renewable Power Generation, IET*, 7(1), 36–44. [http://doi.org/10.1049/iet-](http://doi.org/10.1049/iet-rpg.2012.0040)  
537            [rpg.2012.0040](http://doi.org/10.1049/iet-rpg.2012.0040)

538    Taylor, K. E. (2005). Taylor Diagram Primer, (January), 1–4. <http://doi.org/10.1029/2000JD900719>

539    World Meteorological Organization. (2011). *Guide to Climatological Practices WMO-No. 100.*  
540            <http://doi.org/WMO-No. 100>

541    Zubiate, L., McDermott, F., Sweeney, C., & O'Malley, M. (2016). Spatial variability in winter NAO-  
542            wind speed relationships in Western Europe linked to concomitant states of the East Atlantic  
543            and Scandinavian Patterns. *Quarterly Journal of the Royal Meteorological Society*.  
544            <http://doi.org/10.1002/qj.2943>

545